Image Fusion

Werner Backfrieder[1], Rudolf Hanel [2], Markus Diemling[1,3], Thomas Lorang[4], Joachim Kettenbach[2], Herwig Imhof[2]

[1] Department of Biomedical Engineering and Physics, University of Vienna, Austria
[2] Department of Radiology, Vienna University Hospital, Austria
[3] Department of Nuclear Medicine, PET Centre, Vienna University Hospital, Austria
[4] Department of Medical Computer Science, University of Vienna, Austria

Corresponding author:
Werner Backfrieder
Department of Biomedical Engineering and Physics
University of Vienna
Vienna University Hospital 4L
Waehringer Guertel 18-20
A-1090 Vienna
Austria

Email: werner@bmtp.akh-wien.ac.at
Phone: +43-1-40400-3983
Fax: +43-1-40400-3988

Introduction

In modern radiology imaging modalities for three-dimensional medical visualisation of anatomy and function are in clinical use. Various physical quantities measured by the interaction of e.g. x-rays, magnetic fields or ultra sound with the human body provide modality inherent information about the human body, in general information is complimentary.

For instance, a 3D map of physiological processes is reconstructed in positron emission tomography (PET). Specific radio-chemicals label metabolic processes by the emission of positrons (β^+-particles). The positrons are localised by the detection of the coincident photons emitted in opposite directions after electron-positron annihilation.

Magnetic resonance imaging (MRI) uses nuclear spin interaction with the magnetic field and resonance phenomena to generate an image of the tissue of the human body.

Computed tomography (CT) uses the absorption of x-rays on its way through the body to reconstruct a 2D image of the absorption coefficients within an axial slice. Stacks of slices are used to get a fully 3D image of the body.

PET however shows physiological processes but little anatomical information, MRI in general proton densities of the human body and CT highly detailed anatomical information on the distribution of absorption coefficient, with high contrast in bone but little in soft tissue.

Image fusion is applied for local integration of complimentary information in multi modality images for use in diagnostics and therapy planing. For example, to add anatomical information from MR to the physiological information of PET, or to add information on the soft tissues from MRI to the information on bony structures from CT. Possible applications are comparing pre- and post-therapeutic images in order to evaluate treatment or image fusion in image-guided surgery, where the surgeon's view is overlaid by a preoperatively prepared feature model. This allows the surgeon to look beyond the skin, or to control immediately the performance with respect to the preoperatively planned surgery.

The problem which image fusion faces, assuming consistent reconstruction, disregarding problems coming from distortions in medical imaging, is how to align the 3D data sets accurately. Depending on the modalities and the anatomy in the region of interest, alignment is obtained manually or automatically. Both means to compare the grey values of volume elements (voxels) in each modality, which allow the computation of the appropriate matching transform. The simplest case to consider is rigid misalignment, which can be compensated by translation and rotation of the rigid volume. Most likely the situation is more sophisticated, as for instance the physical volumes that are mapped in diverse modalities cannot necessarily be aligned by rigid transforms, since the patient most likely is not in the same position during both acquisitions or the post operative anatomy has changed. This may lead to deformations of tissue, which have to be considered in the image matching algorithm, either as a linear or non-linear model.

Principles of image fusion

The representation of complimentary information in multi-modality imaging, is achieved by fusion (registration). Respective anatomical structures are matched against each other to visualise for example functional information from PET together with anatomical structures from MRI. Generally image volumes acquired in different modalities have different slice positions and orientation, furthermore corresponding tissue types in general differ in grey values or are not visible at all. Thus simple com-

parison of plain image slices is not possible. Complex mathematical algorithms are used for image fusion under user control or fully automated applications were developed for special anatomical sites and modalities.

A registration procedure is considered as a four steps procedure.

- Identification of relevant features in both volumes to be matched (segmentation, classification)
- Minimisation/maximisation of a cost function indicating the degree of alignment between the images. The cost function is defined using the identified features.
- Transformation (reformatting) of the data sets to match each other in scale and position.
- Representation of data
  The human interpreter needs a presentation of registered images in an intuitive way. There exist various display methods optimised for diagnosis, biomedical image evaluation, surgical planing and navigation. Application dependent relevant features are emphasised or both image data are shown in full detail without any abstraction.

[Figure 1]

As an example for the above registration scheme the matching of two rectangles, as shown in figure 1, is discussed. A simple matching method, point-to-point matching, is used. Three corresponding points at the corners of each rectangles are defined as features and ordered into pairs (A,A‘), (B,B‘) and (C,C‘). Each of the pairs contains one point on both rectangles. In this case the cost function is the sum of the distances of the point-pairs. There exist various methods to solve the problem. In this simple case the parameters for rotation and translation are estimated in one step, solving a system of mathematical equations. The iterative estimation of the matching parameters provides an alternative solution to the problem. Alternating incremental translations and rotations are performed before the evaluation of the cost function. Optimal registration is given when an extreme value of the cost function is found. A multi-scale approach could speed up the procedure. There a coarse parameter estimate is refined in every iteration step. Iteration is terminated when a tolerance limit is reached.
With the matching parameters a transform matrix is computed, reflecting the mathematical relation between the base and matching image. The matching image is transformed to the grid of the base image using this matrix. Since reformatted pixels of the matching image generally lie between the grid points of the base image interpolation is necessary. Linear interpolation is fast and mostly provides sufficient accuracy. For high image quality spline or windowed sinc interpolation is used at the cost of higher computational efforts and interpolation artefacts, e.g. distortion of sharp edges due to over oscillation.
In this simple case it is sufficient to show the base and reformatted matching image side by side on the screen or together with a transparent overlay of both. For more complex anatomical sites or in surgical planing and navigation an abstract three dimensional (3D) display is generated. Organs (objects) from both image volumes are merged and the image volume is rendered in transparent 3D mode.

Segmentation

In a way the concepts of image fusion or registration need reliable definition of image inherent features. These features are prepared by segmentation or classification. In the simplest case features are landmarks, where at least three distinct landmarks are needed to register two image volumes in 3D. These are minimum requirements, since inaccurate definition of even one landmark inevitably leads to registration errors. To achieve redundancy more than three landmarks are chosen, what is done in simple manual registration procedures.

There is no general solution for segmentation of medical images. It is reported, that manual segmentation has large variability (Kaus et al. 1998, Warfield et al. 1998). Warfield and Kikinis report 15 % variability in the segmentation of cortical grey matter of the brain doing segmentations by five different experts. Kaus reports 15-20 % variability in segmentation of brain tumours by multiple experts. Automated segmentation techniques, designed for special problems, would decrease operators bias in segmentation results, as for instance in applications developed for neuro radiology (Nakajima et al. 1997).

There is a great variety of segmentation algorithms (Pal et al. 1993), incorporation different levels of automation: manual thresholding, semiautomatic region growing, morphological operations and multi-spectral methods like clustering methods or neural networks (Specht 1990). Since multi spectral methods require registration of spectral images, these algorithms are implemented using an iterative procedure. In each iteration images are classified and registered until sufficient overlay is achieved (Collins et al. 1992). Classification algorithms need prior information from training sets of each tissue type. These training sets are defined either manually or by a rough preclassification, e.g. a geometrical model.

After segmentation features are extracted for input into the registration algorithm.

In general results of automated segmentation are reproducible, since most algorithms are deterministic. From grey level images anatomical structure have to be extracted like a human expert would do. Due to restrictions inherent to the imaging modality, e.g. resolution, imaging artefacts, partial volume effect, image inhomogeneities, external information has to be implemented (Dellepiane et al. 1995). This external or a priori information is either structural or functional and is called domain information. With segmentation techniques under operator control decisions employing domain information on complex anatomical features are implicitly drawn by the human expert. But in an automated procedure this domain knowledge needs to be formulated by a mathematical rule set.

Knowledge based algorithms incorporate domain information to achieve further automation. Questions are answered checking some model in the knowledge domain (Wells III et al. 1996). Questions on the grey-level distribution of some structure within the image are checked using intensity models (Vannier et al. 1985). Questions on the characteristics of the imaging modality, that was used to acquire the image, are checked by imaging models (Wells III et al. 1996). Shape models, dealing with questions of shape, like the average curvatures of anatomic features in the healthy adults, are used for biasing predictors (Szekely et al. 1996). Finally there are geometric models for the description of spatial relationship in structures, like ”where feature **A** branches feature **B** is expected to be in near vicinity”(Gibbs et al. 1996).

A simple intensity model is the Gaussian classifier. The likely-hood of a voxel beeing a member of a specific tissue class is estimated by evaluating Gaussian probability distributions derived from representative grey values for each tissue type from predefined training sets. More sophisticated models will include higher orders of stochastic relations between not only voxels but contiguous regions (Westin et al. 1998).

The imaging models have to contain information on geometrical distortions of the image intrinsic to the acquisition device as well as reconstruction artefacts and the grey value bias that may systematically be superimposed on images. Commonly the procedures needed for dealing with these kind of phenomena are not included in the segmentation task, but are performed in an preprocessing step (Wells III et al. 1996). Although recognition of shape cannot be formulated with exact mathematical rules, a class of shape models proofed to be useful during last years: combinations of deformable models and principal component analysis (Szekely et al. 1998, Kaus et al. 1998). The models are used in general to uniquely segment structures, which were left unclassified by the intensity models.
To achieve ”objective” and reproducible segmentation, reducing operator interaction the combination of grey level based classifiers together with sophisticated geometrical models is a prospering field of research.

Registration in clinical applications

In (Maintz et al. 1998) a general framework of medical image registration is given. We want to focus on intra-subject, inter-modality matching, i.e. image data from the same subject acquired in several modalities. There rigid and elastic transforms are of clinical relevance (Hata 1998, Hata et al. 1998). Assuming no deformation of the object the image volumes are related using a model for motion of rigid bodies. A global transform matrix with 9 parameters (respectively 3 for translation, rotation and scaling) is used for matching in 3D space. These methods are computationally fast and show sufficient accuracy, especially in the head region. Machine inherent distortions in MR images are compensated using complex hydro-mechanical models for inter-modality matching. There are several application for matching functional EPI images to anatomical T1 weighted images in MR or the fusion of emission CT images with MR (Levin et al. 1989).
In the following the concepts of two method using rigid transforms are discussed in detail.

Chamfer matching

In the group of rigid transform methods chamfer matching is a surface-to-points matching algorithm. The matching features are the surfaces of the same object in both image volumes. By segmentation these features are identified. The accuracy of the final matching is strongly dependent on careful feature segmentation. There exists no general automated segmentation procedure applicable to all anatomical sites of the human body. Semi-automated, grey level based methods as region growing are commonly used. Under operator control regions of interest (ROIs) are defined around manually selected seed points by adjusting upper and lower thresholds of grey values of pixels contained in the region. Region growing can be controlled by manually drawing limits to separate neighbouring structures with similar grey values. A higher degree of automation can be achieved with morphological operations prior to region growing (Höhne et al. 1990). By erosion small connections between neighbouring organs with a similar range of grey values are removed. The focused organ is selected by region growing and a final dilation step is applied to compensate for the erosion. This procedure was used for the segmentation of the brain in MR images (Robb 1995, Serra 1982).
Defining the cost function, the surface of the segmented organ in the base volume is extracted and a set of random points on the respective surface in the matching volume is selected. The cost function gives the summed distance of the point set from the base surface. Computational efficacy is increased by using a surface to distance

map. To every voxel position in the base volume the distance to the closest surface point is assigned. Distances are calculated using the efficient chamfer algorithm (Borgefors 1988). In an iterative algorithm the point set is moved over all possible locations in the distance map. The global minimum of the cost function marks the position of best matching. A multi scale approach further speeds up the matching procedure (Soltanian-Zadeh et al. 1994, Moktharian et al. 1999).

Mutual information matching

Given the problem of registering two different MR image volumes of the same individual. When perfectly aligned the grey values of corresponding voxels are nearly the same. Differences are due to noise. With multi modality images different tissue types show characteristic ranges of grey values, inherent to the modality. Simple similarity measures as squared difference of voxel values or correlation are not sufficient in that case for use in a cost function. A more general measure, mutual information, reflecting the statistical properties of data, shows the correlation of tissue types in different modalities.

The cost function used for registration of the reference and matching volume maximises the mutual information of all voxels in an image volume. This is a statistical measure, defined in terms of entropy. Entropy can be interpreted as the degree of uncertainty, variability, or complexity in a random variable. If images are in perfect registration every voxel in both images should belong to the same specific tissue type. The co-occurrence matrix (two dimensional histogram) shows distinct clusters for each tissue type. If images are not registered clusters are blurred, since voxels at corresponding locations in both volumes belong to different tissue classes. The degree of blurring is estimated by mutual information. A statistical standard method, Parzen windowing, is used to estimate the entropy density function from the discrete samples in the co-occurrence matrix. Accounting for noisy data in finding the global maximum, noisy derivative estimates are used in the gradient ascension procedure to exclude local maxima (Gangolli et al. 1983, Warfield et al 1998., Collins 1994). Accelerating the search for the maximum a multi scale approach is implemented, where the search is done with a coarse to fine method. Maxima found on the coarse grid are used as initial guesses on the finer grid in the next step.

The method works automatically and direct on medical images, in contrast to other methods that require the setting of fiducial markers or some other types of manual interaction for registration. Thus, the algorithm is suitable for intra operative registration, where stability and simplicity are desirable.

Furthermore this type of cost function is flexible to be used with a deformable registration method. Several groups of investigators (Gee et al. 1993) reported the cost function can be formulated as the sum of a voxel similarity and an elastic regularisation energy term, so that the general problem of registration is to minimise the matching energy function. For elastic deformations the potential energy of the object deformed by an external force is measured.

Clinical applications

Interactive registration of MR and CT volumes

Interactive methods allow physicians to gain complete control over the registration process. Matching volumes may be translated, rotated and scaled with respect to a phase volume. Rotations, translations and scalings of the base volume are mapped to the matching volume. A framework for fast reformatting of oblique slices gives immediate feedback of rigid body transformations to the physician by overlaying transparent images of the matching volume onto images of the base volume in multiplanar

reconstructions. This allows for easy correction of patient-related mis-alignment, provided both volumes have the same slice orientation.
Different slice orientations require physicians also to handle image inherent mis-alignments. However, most modern imaging modalities supply header information containing the orientation for each slice; this information is standardised in DICOM 3.0. Further information like pixel dimensions and slice distance, location and thickness allow for an automated registration of equipment related – or series related – geometrical parameters. In this way, axial slices are automatically reconstructed out of volumes composed of sagittal slices, and this reconstructed volume may be registered to a base volume composed of axial slices again. Especially the scaling between both volumes is completely determined by the pixel dimensions in the header information fields.

[Figure 2]

Interactive registration methods commonly suffer from a subjective validation of registration processes. Their main advantages are intuitive handling, immediate display of results and the fact that they do not need any time consuming pre-processing. Figure 2 shows the user interface of the software developed at the Vienna University Hospital. The result achieved by a registration of an axial MR (256 * 256 * 21, 0,976 mm voxel dimensions) and an axial CT (512 * 512 * 46, 0,625 mm pixel dimensions) are displayed. To visualise the degree of alignment the contour of bones from the CT is overlaid in the MR image.

CT-SPECT registration
Diagnosis and therapy of malignant carcinomas in the oral cavity, e.g. squamous cell carcinoma, is based on accurate information about tumour extension, infiltration of adjacent tissue and metastasises in lymph nodes. Since CT provides detailed anatomical information but no functional information, accurate differentiation of infiltrated cancerous tissue is difficult. In SPECT accumulation of a tumour-specific radioactive marker is imaged. Glands are shown together with pathological changes in tissue. Spatial fusion of CT and SPECT images enables accurate tumour diagnosis.

[Figure 3]

The example shows a patient with a squamous cell carcinoma of the oral cavity in the head and neck region. 3D-CT image data were obtained on a Philips Tomoscan SR7000 (120kV, 400mA), 512x512 pixel/slice, 3mm slice thickness, FOV=185mm, using an iodic contrast medium. ^{99m}Tc Sestamibi szintigrams were acquired on a Picker Prism3000, 128x128 pixel/slice, 3.6mm slice thickness, FOV=46cm. For spatial registration of the images chamfer matching was used. Semiautomatic segmentation (region growing, manual tracing) was used to define the surface of the glandula parotis and the opposite glandula submandibularis in respective volumes of both imaging modalities. Figure 3 shows the segmented glands in both modalities, red in CT and green in SPECT. Figure 4 schows a semitransparent overlay of the registered CT and SPECT image. Activity is shown in the glands and in the tongue where the tumour is located.

[Figure 4]

Sufficient registration of anatomical structures and functional information was achieved. The mean distance between corresponding surfaces was about 4 pixel, i.e. 2.8mm. This calculated value is worse than observed spatial overlap, since glands are overemphasised in SPECT, because of imaging artefacts and rigid filtering of reconstructed scintigraphic images.
Semiautomatic registration provides a tool for simultaneous representation of anatomic and functional information and thus improves accuracy in tumour staging in the complex anatomical site of the oral cavity and the neck.

MRI-CT registration in ENT surgery
In ear-nose-throat (ENT) surgery minimally invasive methods have been established during the last decade. Since the area of surgery is not open, the surgeon cannot look directly on the surgical target. Optical devices are used to control surgical instruments in small body cavities. Experienced surgeons have to interpret distorted images provided by the fish eye optics of the endoscope. Besides image distortions navigation in the surgical field is complicated by humidity of the patients breath and blood covering the lens. Under these facts sensitive structures like nerves and blood vessels must not be injured to prevent the patient from severe harm.

[Figure 5]

Modern radiology with high resolution 3D imaging from MR and CT together with medical computer science is the basis for surgical planing and intra surgical navigation. Images from both CT and MR are fused to show both soft tissue, nerves, blood vessels and bone in high detail. Figure 5 shows the fusion of a MR and CT data set. Data are reformatted to the grid of the CT images. A transaxial slice through the head is shown. Bone, invisible in MR, is coloured yellow. Since surgical planing and navigation needs more than in-plane information a 3D display mode was developed. Critical structures were segmented from MR images and imported to the CT volume. Colours were assigned to the anatomical object and the whole scenery was visualised using transparent 3D rendering. Figure 6 shows a transparent gradient shading from a skull. The optical nerve is yellow, the arteria carotis is red and the tumour green. With transparent rendering the surgeon can see behind surfaces anf gets an impression about the relative distances between objects. With special hardware, like 3D goggles, a real 3D view by stereoscopic rendering can be generated.

MRI-PET registration
For the clinical application of multi modal image fusion it is desirable to have tools available that require minimum operator interaction. An application performing multi modal image registration of brain scans without user interaction was developed. It has the advantages of full 3D support and short processing time. The tool is clinically used for the co-registration of PET-MR and SPECT-MR images.
The software presented performs image registration using the normalised mutual information algorithm from the ‚AnalyzeAVW‘ library (Biomedical Imaging Resource, Mayo Foundation, Rochester, MN). This algorithm maximises the degree of dependence of two variables by means of the Kullback-Leibler measure (Viola 1995, Viola et al. 1995). No prior manual segmentation of the volumes is necessary.

[Figure 7]

Figure 7 shows the input and the output windows of the fusion tool. A MRI scan from a patient suffering from temporal lobe epilepsy was fused to the corresponding PET scan for the anatomical identification of pathological PET foci.
The MR scan was acquired on a Philips Gyroscan at 1.5 T using a FLAIR sequence with a slice thickness of 4 mm, image matrix of 256 x 256 and a FOV of 23 cm.
The PET FDG image was acquired on a GE Advance, attenuation corrected and reconstructed with a slice thickness of 4.25 mm, image matrix of 128 x 128 and a FOV of 40 cm. For display, all images are interpolated to 200 x 200 x 70 voxel grid.
As a result of fusion, the two volumes are presented after registration as well as a colour coded overlay of both.

Acknowledgements
Authors would like to thank the Clinic of Nuclear Medicine, the PET Centre, the Department of Neuroradiology and the Clinic of ENT diseases of the Vienna University Hospital for providing image data. This work was partially supported by the grant P12463-MED of the Austrian Science Fund.
.

References

1. Borgefors G., (1988) Hierarchical chamfer matching: A parametric edge matching algorithm, IEEE Trans. Pattern Anal. Machine Intell. 10:849-865

2. Collins D.L., Peters T.M., Dai W., Evans A.C., (1992) Model based segmentation of individual brain structures from MRI data." SPIE Proceedings of 1st International Conference on visualisation in Biomedical Computing 1808:10-23

3. Collins D.L., (1994) 3D Model-based segmentation of individual brain structures from magnetic resonance imaging data. PhD thesis, McGill University

4. Dellepiane S., Fontana F., (1995) Extraction of intensity connectedness for image processing, Pattern Recognition Letters 16:313-324

5. Gangolli, A.R., Tanimoto, S.L., (1983) Two pyramid machine algorithms for edge detection in noisy binary images, Information Processing Letters 17:197-202.

6. Gee, J.C., Reivich, M., Bajcsy, R., (1993) Elastically deforming 3D atlas to match anatomical brain images. J. of Compt. Assist Tomogr 17:225-236

7. Gibbs P., Buckley D.L., Blackband S.J., Horsman A., (1996) Tumour volume determination from MR images by morphological segmentation, Physics in Medicine and Biology 41:2437-2446

8. Hata N. (1998) Rigid and deformable medical image registration for image-guided surgery, PhD thesis, University of Tokyo.

9. Hata N., Dohi T., Warfield S., Wells W., Kikinis R., Jolesz F.A., (1998) Multimodality deformable registration of pre- and intraoperative images for MRI guided brain surgery;
http://splweb.bwh.harvard.edu:8000/pages/papers/noby/miccai98/hata192.htm

10. Höhne K. H., Hanson W. A. (1990) Interactive 3D-segmentation of MRI and CT volumes using morphological operators. Journal of Computer Assisted Tomography 10:41-53

11. Kaus M., Warfield S., Jolesz F., Kikinis R., (1998) Adaptive template moderated brain tumor segmentation in MRI. Bildverarbeitung für die Medizin, Springer Verlag pp. 102-106

12. Levin D., Hu X., Tan K.K., Galhotra S., Pelizzari C.A., et al. (1989.) The brain: Integrated three-dimensional display of MR and PET images. Radiology 172:783-789

13. Maintz A., Viergever M. (1998) A survey of medical image registration. Medical Image Analysis 2 (1): 1-36

14. Mokhtarian, F. Suomela R., (1999) Curvature scale space for image point feature detection, Proc. International Conference on Image Processing and its Applications, Manchester, UK,: 206-210,

15. Nakajima S., Atsumi H., Kikinis R., Moriarty T.M., Metcalf D.C., Jolesz F. A., Black P., (1997) Use of cortical surface vessel registration for image-guided neurosurgery, Neurosurgery, 40(6):1201-1210

16. Pal N., Pal S, (1993) A review on image segmentation techniques, Pattern Recognition 26:1277-1294

17. Robb R.A., (1995) Three-dimensional biomedical imaging: Principles and practice, VCH Publishers Inc. pp.183-188

18. Serra J., (1982) Image analysis and mathematical morphology, Academic Press

19. Soltanian-Zadeh H., Windham J.P., Chen F. (1994) Automated contour extraction using a multi-scale approach, Proceedings IEEE Medical Imaging Conference, Norfolk, VA,

20. Specht D.F., (1990) Probabilistic neural networks, Neural Networks 3:109-118

21. Szekely G., Kelemen A., Brechbuhler C., Gerig G., (1996) Segmentation of 2d and 3d objects from MRI volume data using constrained elastic deformations of flexible Fourier contour and surface models, Medical Image Analysis 1(1):19-34

22. Vannier M., Butterfield R., Jordan D., Murphy W., et al. (1985) Multi-spectral analysis of magnetic resonance images, Radiology 154:221-224

23. Viola, P.A., (1995) Alignment by Maximization of mutual information. Artificial Intelligence Laboratory. Cambridge, MA: Massachusetts Institute of Technology Ph.D. Thesis pp. 155.

24. Viola P.A., Wells III W.M, (1995) Alignment by maximization of mutual information. Fifth International Conference on Computer Vision, IEEE, Cambridge, MA 16-23

25. Warfield S.K. (1998) Real-time image segmentation for image-guided surgery, http://splweb.bwh.harvard.edu:8000/pages/papers/warfield/sc98/index.html

26. Warfield S., Jolesz F., Kikinis R. (1998) A high performance computing approach to the registration of medical imaging data, Parallel Computing 24:11345-1368

27. Wells W.M., Viola P., Atsumi H., S. Nakajima, Kikinis R. (1996) Multi-modal volume registration by maximization of mutual information, Medical Image Analysis 1:35-51

28. Wells III W., Kikinis R., Grimson W., Jolesz F., (1996) Adaptive segmentation of MRI data, IEEE Transactions on Medical Imaging 15(4):429-442

29. Westin C., Kikinis R., (1998) Tensor controlled local structure enhancement of CT images for bone segmentation, Medical Image Computing and Computer Assisted Intervention (MICCAI) 1205-1212

Legends

Figure 1: Registration of two rectangles. Point pairs at the corners of the rectangles are matched by a point-to-point matching algorithm using a rigid body transform.

Figure 2: User interface for manual image registration. A transaxial and sagittal view of the data volume in MR is shown. The overlay shows the contour of the skull bone in the corresponding CT volume. By manual adjustment of rotation and translation images are put to optimal alignment.

Figure 3: Semi-automatic segmentation of the parotic glands in CT and SPECT images. The surfaces of the glands are used to register image volumes by chamfer matching.

Figure 4: Semi-transparent overlay of CT and SPECT images for staging of a squamous cell tumour. The CT image shows anatomical details completed by information of the accumulation of radio pharmaceuticals in glands and tumour tissue.

Figure 5: Fusion of MR and CT images for ENT surgery. The MR image shows high contrast in soft tissue. The matched CT image provides detailed information about bony structures (yellow), which is completely missing in the MR data.

Figure 6: Three dimensional representation of a registered CT and MR data set for use in surgical planing and navigation. Structures of interest were segmented and rendered in transparent mode. The optical nerve (yellow), the carotid artery (red) and the tumour (green) are shown together with the skull.

Figure7: Three panel display of the results of MR-PET matching. The transaxial MR slice is shown in the upper left position. The reformatted PET slice is shown as a grey level image at the lower right position. An overlay of MR and PET images is show at the upper right position. To emphasise functional information from PET a colour representation is used.

Figure1

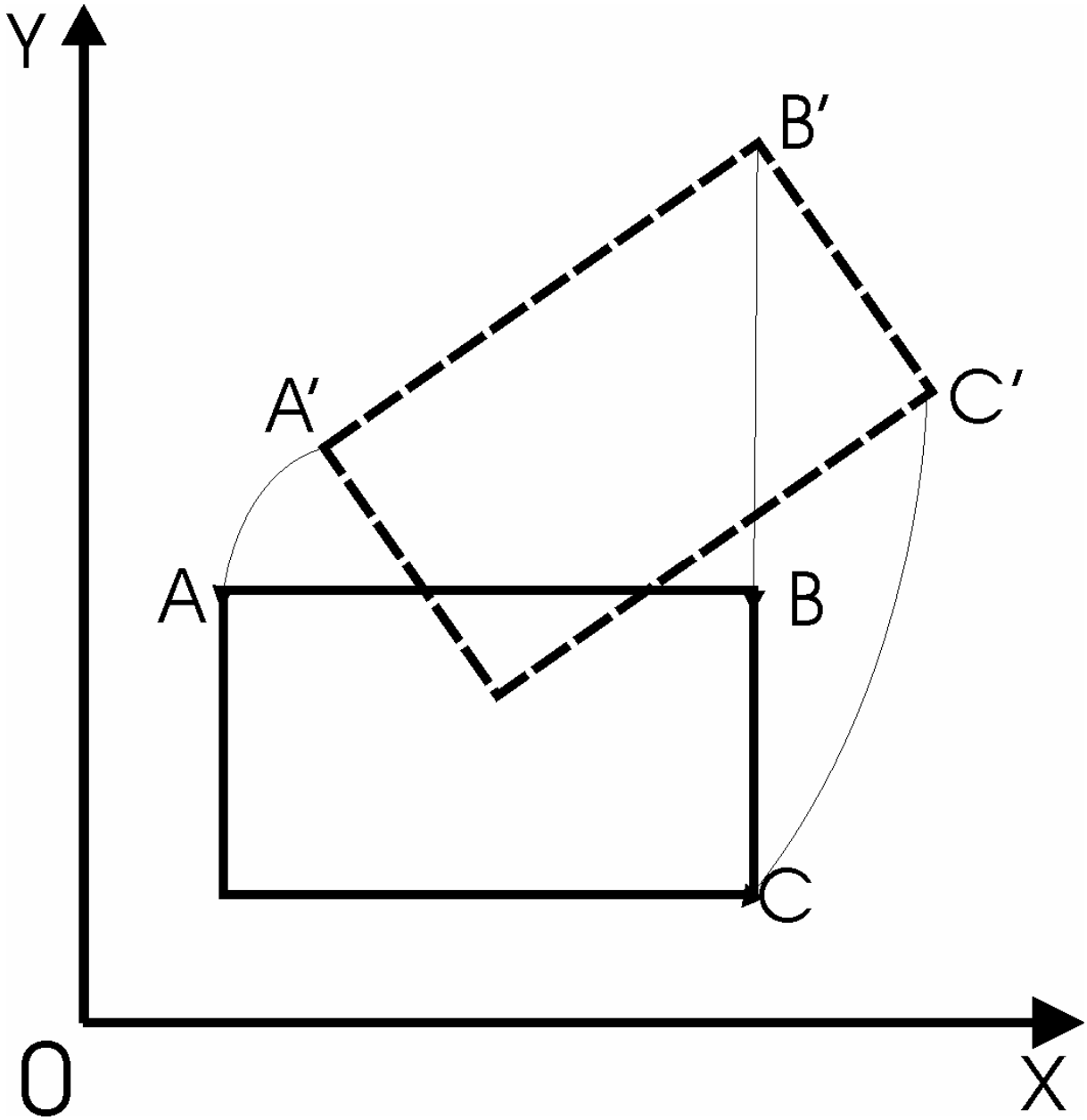

Figure 2

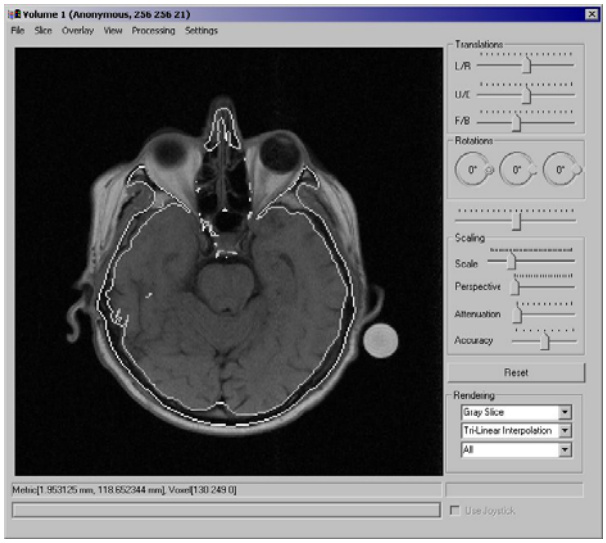
Volume 1 (Anonymous, Z56 Z56 Z1)
File Slice Overlay View Processing Settings
Translations
L/R
U/D
F/B
Rotations
0°
0°
0°
Scaling
Scale
Perspective
Attenuation
Accuracy
Reset
Rendering
Gray Slice
Tri-Linear Interpolation
All
Metric[1.953125 mm, 118.652344 mm], Voxel[130 249 0]
Use Joystick

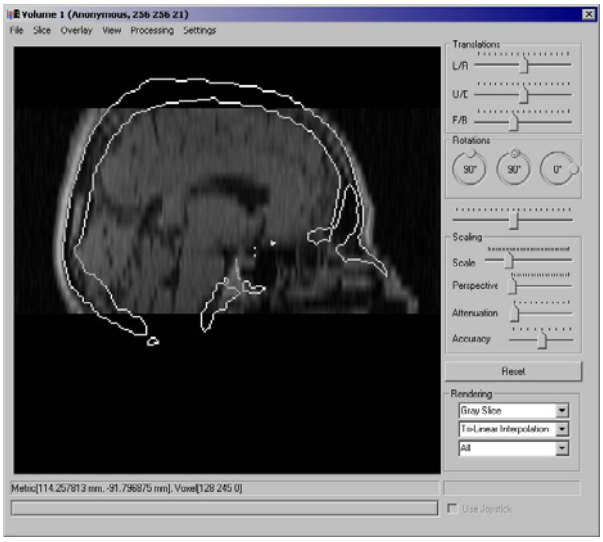
Volume 1 (Anonymous, Z56 Z56 Z1)
File Slice Overlay View Processing Settings
Translations
L/R
U/D
F/B
Rotations
90°
90°
0°
Scaling
Scale
Perspective
Attenuation
Accuracy
Reset
Rendering
Gray Slice
Tri-Linear Interpolation
All
Metric[114.257813 mm, -91.796875 mm], Voxel[128 245 0]
Use Joystick

Figure 3

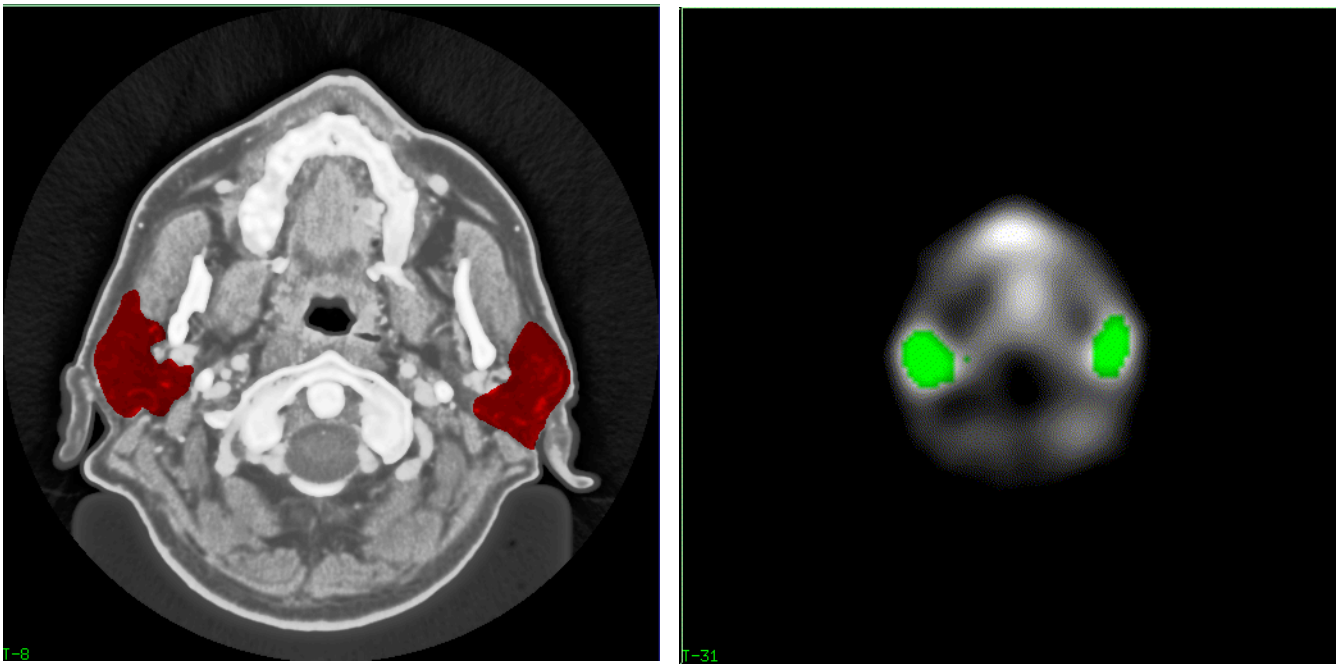

Figure 4

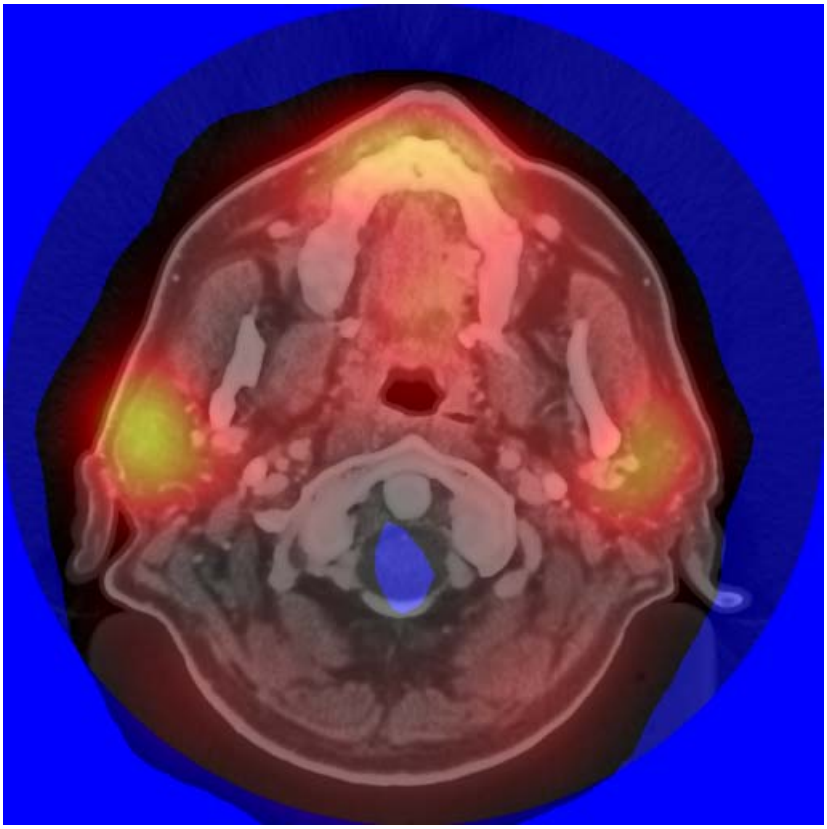

Figure 5

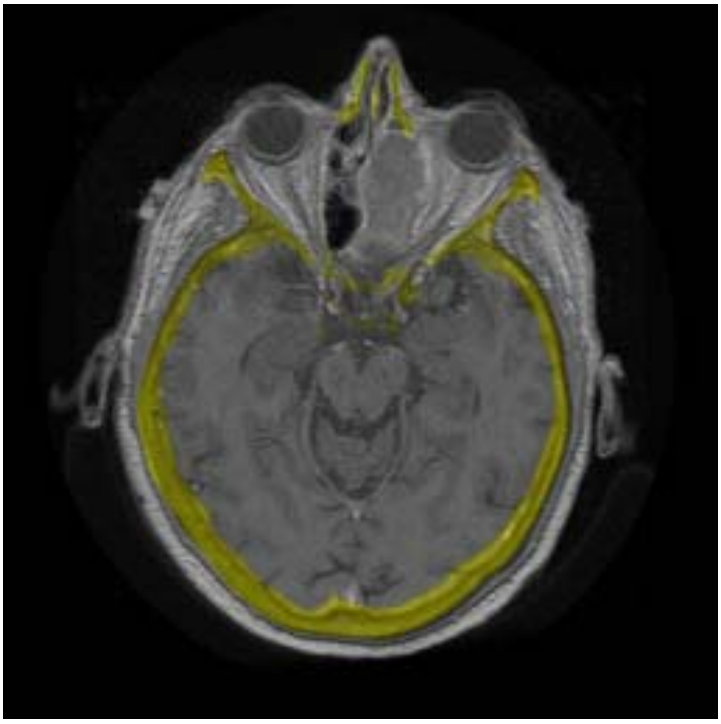

Figure 6:

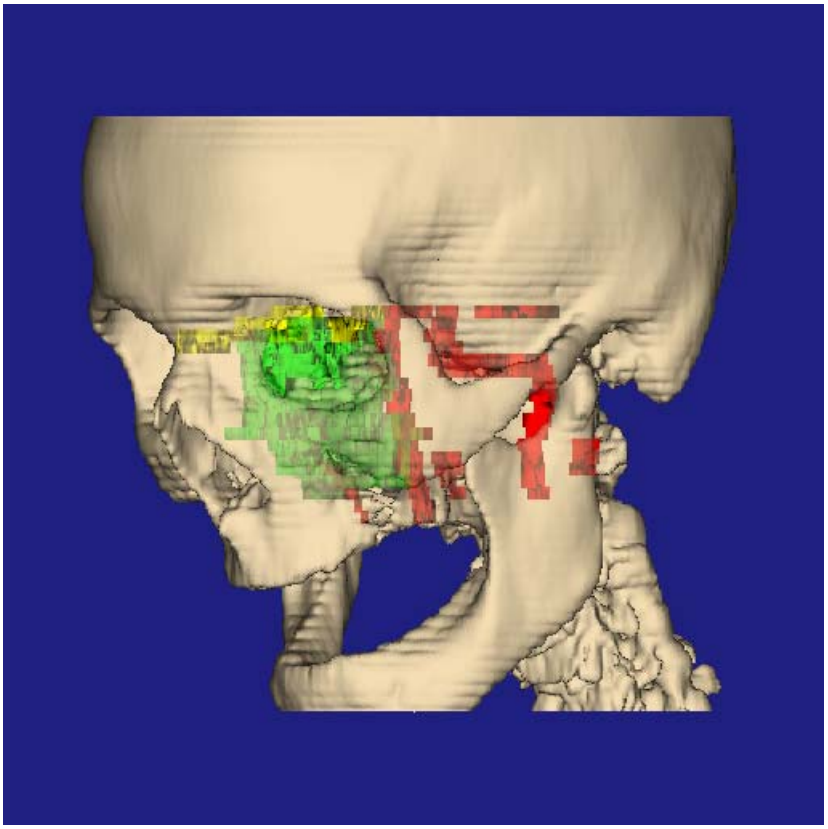

Figure 7